

# Covariance fitting based InSAR Phase Linking

*Phan Viet Hoa VU<sup>1,3</sup>, Arnaud BRELOY<sup>2</sup>, Frédéric BRIGUI<sup>1</sup>, Yajing YAN<sup>3</sup>, and Guillaume GINOLHAC<sup>3</sup>*

<sup>1</sup>ONERA - DEMR, University Paris-Saclay, F-91123 Palaiseau, France

<sup>2</sup>Paris Nanterre University, LEME EA-4416, 92410 Ville d'Avray, France

<sup>3</sup>Savoie Mont Blanc University, LISTIC, F-74000 Annecy, France

## ABSTRACT

This paper proposes an algorithm for phase differences estimation in multi-temporal InSAR. The proposed approach is based on covariance fitting estimation and the majorization-minimization algorithm. Experiments with Sentinel-1 images of Mexico City demonstrate that the proposed approach compares favorably to the state-of-the-art phase linking (i.e., maximum likelihood-based approaches) when the sample support is low (i.e., when the number of pixels in the multi-look window cannot scale with the number of SAR images). Hence, the proposed approach can improve the spatial resolution of phase difference estimation in case of large SAR image time series.

**Index Terms**— Multi-temporal InSAR, Surface Displacement Monitoring, Phase Linking, Least Squares Estimator, Maximum Likelihood Estimator

## 1. INTRODUCTION

Multi-temporal interferometric SAR (MT-InSAR) techniques have been exploited for more than 20 years. Beginning with the concept of Permanent Scatterer Interferometry (PSI) [1, 2, 3] where stable and high coherent point-wise scatterers are exploited to reduce target decorrelation (i.e., temporal and geometrical decorrelation), Distributed Scatterer Interferometry (DSI) approaches were then introduced to increase the estimation density in non-urban area. The first effort to address target decorrelation utilizing randomly distributed scatterers (DS), characterized by shared statistics, is known as Small Baseline Subset (SBAS) [4]. By computing interferograms formed from pairs of images sharing small temporal and spatial baseline, SBAS creates a redundant network of interferograms to retrieve the phase consistency's lost due to the use of spatial/multilook window. SBAS though increases the estimation density, suffers from systematic signal which is short-lived and decays with the temporal baseline [5].

Another popular concept in DSI group is Phase Linking (PL), which “squeezes” all the possible combinations of a time series of  $N$  co-registered Single Look Complex (SLC) SAR images into a vector of  $N - 1$  phase differences (with reference to a single phase) by imposing the phase closure

property. A popular approach consists in properly weighting each interferogram based on target statistics in a maximum likelihood estimation (MLE) scheme [6, 7, 8, 9, 10]. In this setup, an algorithm that we will refer to as MLE-PL performs the phase estimation by solving the MLE of a Gaussian model whose covariance matrix satisfies the phase closure property. The MLE-PL approaches are known to provide a statistically efficient estimator since it is asymptotically unbiased with minimum variance to Cramér-Rao Lower Bound (CRLB). However, this algorithm assumes that the coherence information is known. If not estimated jointly [11, 12], it is usually replaced by a plug-in estimate in practice. This can lead to degraded performance [13], especially when the sample support is low, i.e., when the number of pixels in the multi-look window does not scale well with the number of SAR images in the temporal stack. To mitigate this effect, one usually relies on improved plug-in estimates of the covariance matrix using regularization, such as diagonal loading, or low-rank (LR) approximations [7, 8, 10]. However, these regularizations rely on auxiliary parameters that can be hard to automatically tune in a manner suited to all datasets. A second issue is that MLE-PL relies on a covariance matrix inversion, which can be highly demanding in terms of computational load. This is particularly challenging given the massive volume of short-revisit time and global coverage acquisitions of InSAR imagery provided by many present and upcoming satellite missions.

To address the aforementioned issues, this work considers a counterpart to the MLE-PL formulation through a least-squares covariance fitting formulation (referred to as LS-PL), which has, to the best of our knowledge, not been extensively investigated in the literature. This formulation has the main advantage of not relying on the inverse of the coherence matrix. It can thus avoid inaccuracies due to the poor conditioning of the plug-in estimate without requiring a regularization process. Additionally, we derive a majorization-minimization algorithm to solve LS-PL with a low computational load. Though not enjoying the theoretical asymptotic properties of MLE-PL approaches, experiments in this work will show that the LS-PL formulation compares favorably in terms of computational cost and

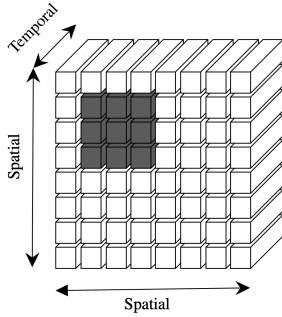


**Fig. 1.** SAR time series datacube representation. Sliding window (in gray)  $\mathbf{x}$  on dataset of the SLC SAR acquisitions.

in performance at low sample support (small spatial window).

## 2. CONVENTIONAL PHASE LINKING VS COVARIANCE FITTING

### 2.1. Multi-temporal InSAR covariance structure

For a multivariate pixel window of  $N$  co-registered SAR images (as represented in Figure 1), we consider a local patch of  $L$  pixels denoted as  $\{\mathbf{x}_i\}_{i=1}^L$ , with  $\mathbf{x}_i \in \mathbb{C}^N$ ,  $\forall i \in [1, L]$ . Assuming that  $\{\mathbf{x}_i\}_{i=1}^L$  is a homogeneous patch of  $L$  pixels sharing the same scattering and statistical properties (i.e. DS characteristics) and thus, the covariance matrix  $\mathbf{C}$ . Given the statistics of interferometric data behavior, the first and second-order moments of  $\mathbf{x}$  are

$$\begin{aligned}\mathbb{E}[x^n] &= 0, \quad \forall n \in [1, N] \\ \mathbb{E}[x^k(x^l)^*] &= v_{k,l} \sigma_k \sigma_l e^{j(\theta_k - \theta_l)}, \quad \forall (k, l) \in [1, N]^2\end{aligned}\quad (1)$$

where

- $\sigma_n^2 = \mathbb{E}[x^n(x^n)^H]$  is the variance of  $x^n$ . We denote the vector of standard deviations  $\boldsymbol{\sigma} = [\sigma_1, \dots, \sigma_N]$ .
- $v_{k,l} \in [0, 1]$  is the coherence coefficient between  $x^k$  and  $x^l$ . We denote  $\boldsymbol{\Upsilon}$  the coherence matrix, with entries  $[\boldsymbol{\Upsilon}]_{k,l} = v_{k,l}$ .
- $\theta_n$  is the phase at instant  $n$ . We denote the phase vector  $\boldsymbol{\theta} = [\theta_1, \dots, \theta_N]$ , and the corresponding vector of complex arguments is

$$\mathbf{w}_{\boldsymbol{\theta}} = [e^{j\theta_1}, \dots, e^{j\theta_N}] \in \mathbb{T}_N, \quad (2)$$

where  $\mathbb{T}_N = \{\mathbf{w} \in \mathbb{C}^N \mid |\mathbf{w}|_i = 1, \forall i \in [1, N]\}$  is the  $N$ -torus of phase-only complex vectors. By convention, to avoid ambiguity, we will use the reference  $\theta_1 = 0$ , which is equivalent to  $[\mathbf{w}_{\boldsymbol{\theta}}]_1 = 1$ .

---

### Algorithm 1 MM algorithm for LS-PL problem (8)

---

```

1: Entry:  $\mathbf{M} \in \mathbb{C}^{N \times N}$ ,  $\mathbf{w}_1 \in \mathbb{T}_N$  (starting point)
2: repeat
3:   Compute  $\tilde{\mathbf{w}}_t = \mathbf{M}\mathbf{w}_t$ 
4:   Update  $\mathbf{w}_t = \mathcal{P}_{\mathbb{T}_N}\{\tilde{\mathbf{w}}_t\}$ 
5:    $t = t + 1$ 
6: until convergence
7: Output:  $\mathbf{w} \in \mathbb{T}_N$ 

```

---

Rewrite the covariance structure in (1) in matrix form, we have

$$\mathbb{E}[\mathbf{x}\mathbf{x}^H] \stackrel{\Delta}{=} \mathbf{C} = \text{diag}(\mathbf{w}_{\boldsymbol{\theta}}) \underbrace{((\boldsymbol{\sigma}\boldsymbol{\sigma}^T) \odot \boldsymbol{\Upsilon})}_{\boldsymbol{\Psi}} \text{diag}(\mathbf{w}_{\boldsymbol{\theta}})^H. \quad (3)$$

This can also be written as a modulus-argument decomposition, i.e.:

$$\mathbf{C} = \text{mod}(\mathbf{C}) \odot \arg(\mathbf{C}) \stackrel{\Delta}{=} \boldsymbol{\Psi} \odot (\mathbf{w}_{\boldsymbol{\theta}}\mathbf{w}_{\boldsymbol{\theta}}^H), \quad (4)$$

### 2.2. MLE-PL problem

Under the common hypothesis that  $\mathbf{x}$  follows a complex circular Gaussian distribution, state-of-the-art PL estimates phase differences  $\boldsymbol{\theta}$  by minimizing the negative log likelihood of the dataset with a given prior estimate of  $\boldsymbol{\Psi}$  as such

$$\mathcal{L}_G(\mathbf{C}) \propto \text{Tr}\{\mathbf{C}^{-1}\mathbf{S}\} + \log|\mathbf{C}| + \text{const.} \quad (5)$$

where  $\mathbf{S} = \frac{1}{L} \sum_{i=1}^L \mathbf{x}_i \mathbf{x}_i^H$  is the sample covariance matrix (SCM) of  $\mathbf{x}$ .

By rewriting (5) with the structure in (4) and assumed known  $\boldsymbol{\Psi}$ , the MLE-PL problem then reads

$$\underset{\mathbf{w}_{\boldsymbol{\theta}} \in \mathbb{T}_N}{\text{minimize}} \mathbf{w}_{\boldsymbol{\theta}}^H (\boldsymbol{\Psi}^{-1} \odot \mathbf{S}) \mathbf{w}_{\boldsymbol{\theta}} \quad (6)$$

In the literature,  $\boldsymbol{\Psi}$  is substituted by an estimate which is the modulus of SCM, i.e.  $\text{mod}(\mathbf{S})$ . [7, 8, 9]. The literature also generally consider the potential use of low-rank regularization to enhance the accuracy of this plug-in (see, e.g., [7]). This approach will be referred to as MLE-PL<sub>LR</sub>.

### 2.3. Least-squares covariance fitting

Notice that MLE-PL relies on a matrix inversion of the SCM, which could be inaccurate at low sample support, as well as computationally demanding. To address these issues, we consider an alternate formulation of the phase estimation problem. Given a plug-in estimate of the covariance matrix, denoted  $\hat{\mathbf{C}}$  that does not satisfy the phase structure as in (4), we seek best projection approach in some sense. First, denote the modulus of  $\hat{\mathbf{C}}$  as

$$\hat{\boldsymbol{\Psi}} \stackrel{\Delta}{=} \text{mod}(\hat{\mathbf{C}}). \quad (7)$$

The least square covariance fitting estimator for the structure in (4) corresponds to the minimization problem

$$\underset{\mathbf{w}_\theta \in \mathbb{T}_N}{\text{minimize}} \quad \|\hat{\mathbf{C}} - \text{diag}(\mathbf{w}_\theta)\hat{\Psi}\text{diag}(\mathbf{w}_\theta)^H\|_F^2 \quad (8)$$

The objective function in (8) is simplified as

$$\begin{aligned} f_{\hat{\mathbf{C}}}^{\text{LS}} &= \|\hat{\mathbf{C}} - \text{diag}(\mathbf{w}_\theta)\hat{\Psi}\text{diag}(\mathbf{w}_\theta)^H\|_F^2 \\ &= -2 \text{Tr} \left( \mathbf{C} \text{diag}(\mathbf{w}_\theta) \hat{\Psi} \text{diag}(\mathbf{w}_\theta)^H \right) + \text{const.} \\ &= -\mathbf{w}_\theta^H (\hat{\Psi} \odot \hat{\mathbf{C}}) \mathbf{w}_\theta + \text{const.} \end{aligned} \quad (9)$$

Denote  $\mathbf{M} = \hat{\Psi} \odot \hat{\mathbf{C}}$ , we can turn the problem into a generic form

$$\underset{\mathbf{w} \in \mathbb{T}_N}{\text{minimize}} \quad -\mathbf{w}^H \mathbf{M} \mathbf{w} \quad (10)$$

A cost-efficient majorization minimization (MM) algorithm [11, 14] is subsequently derived to solve for (9).

Since  $\mathbf{M} \in \mathcal{S}_N^+$ , the quadratic form  $-\mathbf{w}^H \mathbf{M} \mathbf{w}$  is a concave function which is majorized at its tangent  $\mathbf{w}_t$  by its first order Taylor expansion

$$g(\mathbf{w} | \mathbf{w}_t) = -2\Re \left\{ \mathbf{w}^H \underbrace{\mathbf{M} \mathbf{w}_t}_{\tilde{\mathbf{w}}_t} \right\} + \text{const.} \quad (11)$$

Minimizing this surrogate function on  $\mathbb{T}_N$  corresponds to this maximization problem

$$\underset{\mathbf{w} \in \mathbb{T}_N}{\text{maximize}} \quad \Re \left\{ \mathbf{w}^H \tilde{\mathbf{w}}_t \right\} \quad (12)$$

The solution of this problem is the entry-wise projection of the vector  $\tilde{\mathbf{w}}_t$  on a unit complex circle which reads  $\mathbf{w}^* = \mathcal{P}_{\mathbb{T}_N} \{ \tilde{\mathbf{w}}_t \}$ . The resulting MM algorithm to solve for (9) is summed up in the table 1. This MM algorithm is ensured favorable convergence properties [15], notably characterized by a monotonic decrement of the objective function at every iteration.

### 3. REAL DATA

In order to evaluate the performance of the novel LS-PL algorithm, we employed a dataset of SLC Sentinel-1 imagery, acquired between 03/07/2019 and 27/06/2020, encompassing approximately  $14 \times 22 \text{ km}^2$  around Mexico City which is known for its substantial subsidence rate [16]. To better access to the signal decorrelation effect on the dataset, we apply 3 approaches (i.e., MLE-PL, MLE-PL<sub>LR</sub>, and LS-PL) with a sliding window of  $L = 64$  pixels on a short temporal baseline of 15 acquisitions and a longer temporal baseline of 31 acquisitions, with a temporal resolution of 12 days. Figures 2 and 3 present the results for  $N = 15$  and  $N = 31$  dates, respectively.

We observe that MLE-PL provides a noisy output, which is due to its reliance on  $|\mathbf{S}|^{-1}$  (that requires  $L \gg N$  to be

accurately estimated). This can be compensated by the use of a rank-regularized plug-in estimate, as seen from the output of MLE-PL<sub>LR</sub>. Conversely, LS-PL can produce visibly improved interferograms without regularization of  $\mathbf{S}$ , thereby obviating the requirement for additional regularization and parameter tuning.

In parallel, we also notice that MLE-PL and LS-PL are both solved using an MM algorithm with equivalent complexities for each iteration. However, we experienced a faster convergence of LS-PL (roughly 20 iterations needed on average) compared to MLE-PL and MLE-PL<sub>LR</sub> (roughly 200 iterations needed on average). Thus, this formulation appears also advantageous in terms of computational time.

## 4. DISCUSSION AND CONCLUSION

In this study, we proposed an alternate formulation of phase linking through a least-squares fitting of a phase-structured covariance matrix, rather than the more usual MLE approach. An MM algorithm was proposed to compute the corresponding phase estimates. Experiments on real world InSAR data in terms of accuracy at low sample support, and computational load.

## 5. REFERENCES

- [1] Alessandro Ferretti, Claudio Prati, and Fabio Rocca, “Non-linear subsidence rate estimation using permanent scatterers in differential SAR interferometry,” *IEEE Transactions on Geoscience and Remote Sensing*, vol. 38, no. 5, pp. 2202–2212, 2000.
- [2] Alessandro Ferretti, Claudio Prati, and Fabio Rocca, “Permanent scatterers in SAR interferometry,” *IEEE Transactions on Geoscience and Remote Sensing*, vol. 39, no. 1, pp. 8–20, 2001.
- [3] Bert M. Kampes, *Displacement parameter estimation using permanent scatterer interferometry*, Ph.D. thesis, Delft, Netherlands, 2005.
- [4] Paolo Berardino, Gianfranco Fornaro, Riccardo Lanari, and Eugenio Sansosti, “A new algorithm for surface deformation monitoring based on small baseline differential SAR interferograms,” *IEEE Transactions on Geoscience and Remote Sensing*, vol. 40, no. 11, pp. 2375–2383, 2002.
- [5] Homa Ansari, Francesco De Zan, and Alessandro Parizzi, “Study of Systematic Bias in Measuring Surface Deformation With SAR Interferometry,” *IEEE Transactions on Geoscience and Remote Sensing*, vol. 59, no. 2, pp. 1285–1301, 2021.
- [6] Andrea Monti Guarneri and Stefano Tebaldini, “On the Exploitation of Target Statistics for SAR Interferometry Applications,” *IEEE Transactions on Geoscience and Remote Sensing*, vol. 46, no. 11, pp. 3436–3443, 2008.
- [7] Alessandro Ferretti, Alfio Fumagalli, Fabrizio Novali, Claudio Prati, Fabio Rocca, and Alessio Rucci, “A New Algorithm for Processing Interferometric Data-Stacks: SqueeSAR,” *IEEE*

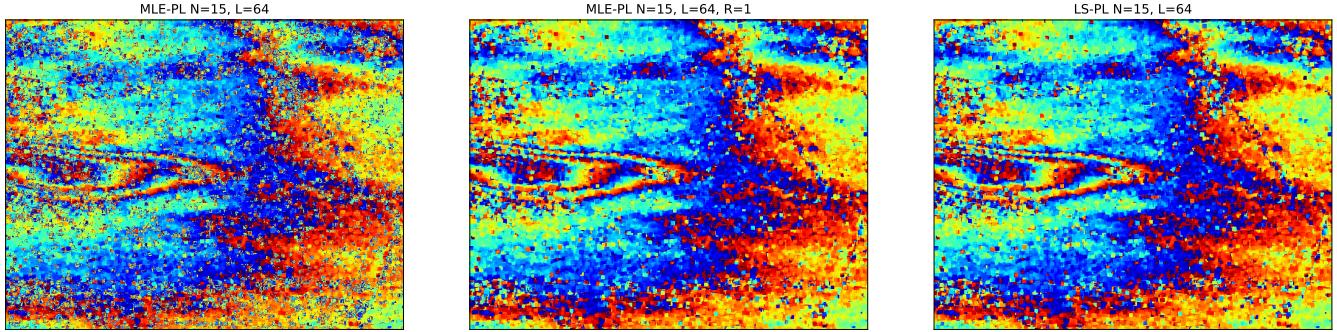


**Fig. 2.** A focused view of the longest temporal baseline interferogram (Jul 3, 2019 - Dec 18, 2019) estimated with MLE-PL, MLE-PL<sub>LR</sub>, LS-PL (left to right) in case of  $N = 15$  dates and  $L = 64$  pixels using Sentinel-1 data.

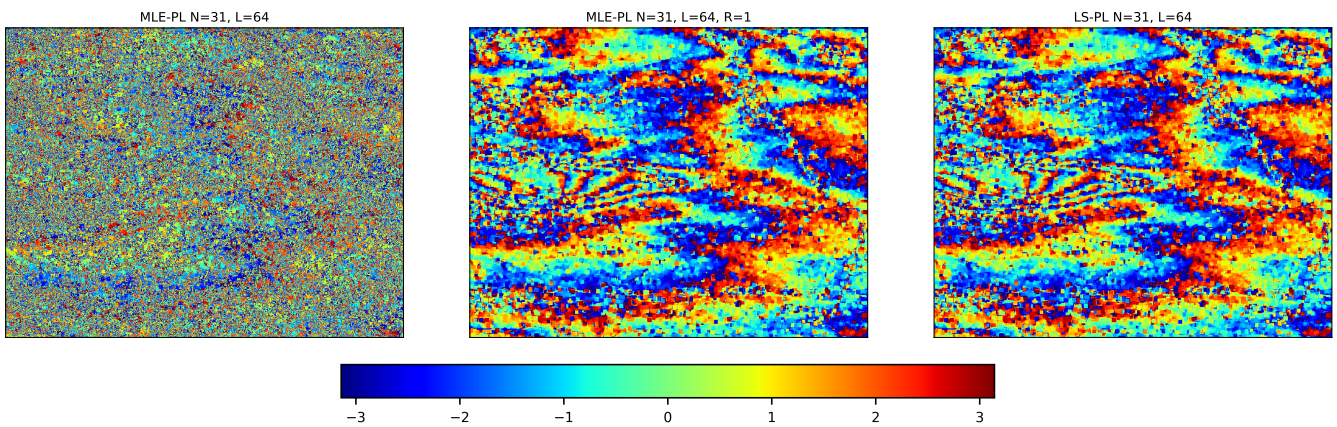


**Fig. 3.** A focused view of the longest temporal baseline interferogram (Jul 3, 2019 - Jun 27, 2020) estimated with MLE-PL, MLE-PL<sub>LR</sub>, LS-PL (left to right) in case of  $N = 31$  dates and  $L = 64$  pixels using Sentinel-1 data.

- Transactions on Geoscience and Remote Sensing, vol. 49, no. 9, pp. 3460–3470, 2011.
- [8] Ning Cao, Hyongki Lee, and Hahn Chul Jung, “Mathematical Framework for Phase-Triangulation Algorithms in Distributed-Scatterer Interferometry,” *IEEE Geoscience and Remote Sensing Letters*, vol. 12, no. 9, pp. 1838–1842, 2015.
- [9] Homa Ansari, Francesco De Zan, and Richard Bamler, “Sequential Estimator: Toward Efficient InSAR Time Series Analysis,” *IEEE Transactions on Geoscience and Remote Sensing*, vol. 55, no. 10, pp. 5637–5652, 2017.
- [10] Homa Ansari, Francesco De Zan, and Richard Bamler, “Efficient Phase Estimation for Interferogram Stacks,” *IEEE Transactions on Geoscience and Remote Sensing*, vol. 56, no. 7, pp. 4109–4125, 2018.
- [11] Phan Viet Hoa Vu, Frédéric Brigui, Arnaud Breloy, Yajing Yan, and Guillaume Ginolhac, “A New Phase Linking Algorithm for Multi-temporal InSAR based on the Maximum Likelihood Estimator,” in *IGARSS 2022 - 2022 IEEE International Geoscience and Remote Sensing Symposium*, 2022, pp. 76–79.
- [12] Chisheng Wang, Xiang-Sheng Wang, Yaping Xu, Bochen Zhang, Mi Jiang, Siting Xiong, Qin Zhang, Weidong Li, and Qingquan Li, “A New Likelihood Function for Consistent Phase Series Estimation in Distributed Scatterer Interferometry,” *IEEE Transactions on Geoscience and Remote Sensing*, vol. 60, pp. 1–14, 2022.
- [13] Ridha Touzi, Armand Lopes, Jerome Bruniquel, and Paris W. Vachon, “Coherence estimation for SAR imagery,” *IEEE Transactions on Geoscience and Remote Sensing*, vol. 37, no. 1, pp. 135–149, 1999.
- [14] Mojtaba Soltanalian and Petre Stoica, “Designing unimodular codes via quadratic optimization,” *IEEE Transactions on Signal Processing*, vol. 62, no. 5, pp. 1221–1234, 2014.
- [15] Meisam Razaviyayn, Mingyi Hong, and Zhi-Quan Luo, “A Unified Convergence Analysis of Block Successive Minimization Methods for Nonsmooth Optimization,” *SIAM on Optimization*, vol. 23, no. 2, pp. 1126–1153, 2013.
- [16] Yajing Yan, Marie-Pierre Doin, Penélope Lopez-Quiroz, Florence Tupin, Bénédicte Fruneau, Virginie Pinel, and Emmanuel Trouve, “Mexico City Subsidence Measured by InSAR Time Series: Joint Analysis Using PS and SBAS Approaches,” *IEEE Journal of Selected Topics in Applied Earth Observations and Remote Sensing*, vol. 5, no. 4, pp. 1312–1326, 2012.